Cell. Mol. Life Sci. 63 (2006) 1899–1905
1420-682X/06/161899-7
DOI 10.1007/s00018-006-6183-7

Cellular and Molecular Life Sciences

Research Article

Stability analysis of the bacteriophage ϕKMV lysin gp36C and its putative role during infection

Y. Briers [a, *], R. Lavigne [a], P. Plessers [a], K. Hertveldt [a], I. Hanssens [b], Y. Engelborghs [c] and G.Volckaert [a]

[a] Division of Gene Technology, Katholieke Universiteit Leuven, Kasteelpark Arenberg 21, Leuven 3001 (Belgium), Fax: +32 16 32 19 65, e-mail: yves.briers@biw.kuleuven.be
[b] Interdisciplinary Research Center, Katholieke Universiteit Leuven Campus Kortrijk, E. Sabbelaan 53, 8500 Kortrijk (Belgium)
[c] Laboratory of Biomolecular Dynamics, Katholieke Universiteit Leuven, Celestijnenlaan 200 D, 3001 Leuven (Belgium)

Received 24 April 2006; received after revision 26 May 2006; accepted 10 June 2006
Online First 17 July 2006

Abstract. The kinetic, thermodynamic and structural stability of gp36C, the virion-associated peptidoglycan hydrolase domain of bacteriophage ϕKMV, is analyzed. Recombinant gp36C is highly thermoresistant ($k = 0.595\ h^{-1}$ at 95 °C), but not thermostable ($T_m = 50.2$ °C, $\Delta H_{cal} = 6.86 \times 10^4$ cal mol^{-1}). However, aggregation influences kinetic stability in an unusual manner since aggregation is more pronounced at 55 °C than at higher temperatures. Furthermore, gp36C reversibly unfolds in a two-state endothermic transition, and circular dichroism analysis shows that gp36C almost completely refolds after a 3-h heat treatment at 85 °C. These properties are in agreement with gp36C being part of the extensible tail which is ejected in an unfolded state during phage infection.

Keywords. PhiKMV, Lysin, kinetic stability, thermoresistance, aggregation, phage infection.

During infection most bacteriophages locally degrade the peptidoglycan (murein) of the host cell in order to inject their genome. Therefore, phages infecting Gram-negative or Gram-positive bacteria often contain muralytic enzymes as part of their injection needle. This virion-associated peptidoglycan hydrolase activity was first observed in the phenomenon of 'lysis from without': T4 phage particles cause premature lysis of the host cell upon infection with high multiplicities [1]. Tail protein gp5 of bacteriophage T4 is responsible for the 'lysis from without' phenomenon due to its muralytic activity during infection [2, 3].

More recently the virion-associated protein gp16 of bacteriophage T7 was shown to enable infection under conditions where peptidoglycan is more extensively cross-linked [4]. Zymogram analysis showed peptidoglycan-degrading activity of gp16 and the prevalence of virion-associated muralytic activities for numerous other bacteriophages infecting Gram-negative or Gram-positive bacteria [5]. In addition, other virion-associated peptidoglycan hydrolases have been experimentally demonstrated in *Escherichia coli* phages T4 [6] and PRD1 [7], *Pseudoalteromonas* phage PM2 [8], *Pseudomonas syringae* phages ϕ6 and ϕ13 [9], *Lactococcus lactis* phage Tuc2009 [10] and *Staphylococcus aureus* phage P68 [11].

We recently reported the functional characterization of the infection-related murein hydrolase domain (gp36C) of bacteriophage ϕKMV, a member of the T7 supergroup infecting the opportunistic pathogen *P. aeruginosa* [12, 13]. This domain is located in the C-terminal of gp36, which is part of the ϕKMV phage particle as shown by liquid chromatography-mass spectrometry [14]. Biochemical characterization of recombinant gp36C confirmed its muralytic activity and revealed an unprecedented kinetic stability. After a heat treatment of

* Corresponding author.

1 h at 100 °C, the enzyme retains more than 50% of its initial activity. Furthermore, after a 2-h heat treatment at 100 °C or autoclaving (15 min at 120 °C, 2 bar), the enzyme still keeps 26% and 21% residual activity, respectively [13].

Interestingly, BLAST analysis revealed that gp36C is most similar to bacteriophage T4 lysozyme (gp *e*), a model enzyme for many stability and folding studies [15]. Despite this similarity, gp *e* shows no intrinsic kinetic stability and is completely inactivated after 5 min at 75 °C [16]. In this respect, the stability of recombinant gp36C offers an interesting comparison to gp *e*.

T4 lysozyme is a small protein (164 amino acids) composed of two lobes connected by a long central α helix C (Fig. 1). The N-terminal lobe has an α/β structure which contains the catalytic triad (Glu11, Asp20, Thr26). The C-terminal lobe is completely α-helical and consists of a cylindrical hydrophobic core. Several substrate-binding residues are present in both lobes [17, 18]. Conformational changes between these lobes that allow accessibility to the catalytic domain are essential for enzymatic activity [19]. Remarkably, comparison of the secondary structure of gp *e* and gp36C reveals the absence of the thermodynamically unstable helix B of gp *e* in the N-terminal lobe of gp36C (Fig. 1) [20, 21]. In gp36C, two of the three essential catalytic residues are conserved (Glu17, Asp26), whereas Ser31 seems to be the functional substitute for the third catalytic residue (Thr26) in T4 lysozyme. Residues that are implicated in recognizing and binding the peptide component of peptidoglycan are conserved in gp36C (Fig. 1). In this study, we describe the kinetic, thermodynamic and structural stability analysis of gp36C.

Materials and methods

Recombinant expression and protein purification. Production of the recombinant fusion protein gp36C-E-His_6 in *E. coli* WK6 {(Δ(*lac-proAB) galE straA nal*^{r} [F′ *lacI*^{q} *lacZ*Δ*M15 proAB*$^+$]} was performed as described previously [13] with minor modifications to allow upscaling. Expression was induced overnight at 16 °C with 1 mM IPTG in 1 l LB medium. Subsequently, the culture was spun down (3300 g, 15 min, 4 °C) and cell pellets were resuspended in 20 ml lysis buffer (10 mM imidazole, 20 mM NaH_2PO_4, 0.5 M NaCl, pH 7.4). This suspension was frozen/thawed four times prior to sonication (3 × 15 s, amplitude 40% on a Vibra Cell, Sonics, Dandurry, Conn.) and filtered successively through 1.22- and 0.45-µm Durapore membrane filters (Millipore, Billerica, Mass). Purification of the recombinant protein was performed on an Äkta FPLC (Amersham Biosciences, Uppsala, Sweden), using a HisTrap HP 1-ml column (Amersham Biosciences). The lysate was loaded after column equilibration with washing buffer (50 mM imidazole, 20 mM NaH_2PO_4, 0.5 M NaCl, pH 7.4; 10 column volumes). The column was washed with 15 column volumes of washing buffer. Protein was eluted in elution buffer (500 mM imidazole, 20 mM NaH_2PO_4, 0.5 M NaCl, pH 7.4) and dialyzed using Slide-A-Lyzer MINI Dialysis units (Pierce Biotechnology, Rockford, Ill.). Protein purity was over 90% as estimated by SDS-PAGE and confirmed by SELDI-TOF analysis, which showed no discernible secondary peaks.

Turbidimetric assays. Substrate for the turbidimetric assay consisted of *P. aeruginosa* (PAO1) cells treated

Figure 1. BLAST alignment of gp36C of phage ϕKMV and gp *e* of phage T4. Gp36C (upper) and gp *e* (below) are aligned (27% identical and 44% similar residues). The catalytic triad is boxed while substrate-recognizing and -binding residues are in bold. The secondary-structure elements are represented by ellipses (α-helices) and arrows (β sheets). Gp36C (dark grey) is a synthesis of the output of PSSM, Porter, PredictProt and PsiPred secondary prediction tools. The secondary structure of T4 lysozyme is based on the crystal structure [14, 15]. Its N- and C-terminal lobes are marked in black and light grey, respectively.

with $CHCl_3$ saturated buffer for 45 min to permeabilize the outer membrane for gp36C [13]. All measurements were performed in 16.7 mM $K_3PO_4 \cdot HCl$ at pH 6.0, the optimal enzyme reaction conditions for gp36C, hereafter referred to as ENZ buffer. Samples of gp36C (11.6 µg/ml; 0.56 µM) were heated at fixed temperatures (between 25 and 95 °C) for 1–10 h and subsequently cooled down on ice for 10 min. After addition of the muralytic enzyme sample (30 µl), the optical density (OD_{600}) of the substrate (270 µl) was followed at 3-min intervals in a Bioscreen C Microbiology reader (Labsystems Oy, Helsinki, Finland) at room temperature as a function of time. All samples were measured in triplicate and were plotted relative to negative controls. The enzymatic activity was quantified in the region of linear descent for each curve. To pinpoint this region, the determination coefficient (R^2) of the linear regression was maximized for an increasing number of measurements in time to ensure the most reliable fit. The corresponding slope is a direct measure for enzymatic activity. Thus, each activity is calculated based on more than 40 data points.

UV-VIS aggregation spectrophotometry. Samples in a dilution series from 1 to 45 µM were heated for 3 h at fixed temperatures (25, 55, 75, 95 °C) and cooled down to room temperature. Two different buffers were used: ENZ buffer and a phosphate-buffered highly concentrated saline solution (20 mM $NaH_2PO_4 \cdot HCl$, 0.5 M NaCl, pH 7.4), hereafter referred to as PBHS. Measurements were performed in a UV-1650PC (Shimadzu, Kyoto, Japan) using 10-mm cuvettes. Gp36C in its native state does not absorb any signal at 350 nm, but upon aggregation it scatters the light beam, thus preventing it from being detected. Therefore, absorption values at 350 and 280 nm were taken as a measure for aggregation and protein concentration, respectively. All samples were vortexed before measurements.

Differential scanning calorimetry. Differential scanning calorimetry (DSC) DSC analyses were performed on a VP-DSC Microcalorimeter (MicroCal, Northhampton, Mass) and analyzed using Microcal Origin (DSC Data analysis in Origin, v5.0; MicroCal). Scans were measured continuously between 10 and 90 °C at 1 °C per minute. Between each individual scan, sample cells were equilibrated for 30 min. Protein samples of 15 and 30 µM were analyzed in ENZ and PBHS buffer.

Circular dichroism. Far-UV circular dichroism (CD) spectra of gp36C (15 µM in PBHS) were recorded after 3-h heat treatments at different fixed temperatures (followed by cooling down to 25 °C) with a Jasco J-810 spectropolarimeter using cuvettes with a path length of 1.00 mm. Spectra were obtained in triplicate at a scan speed of 20 nm per minute and a response time of 1 s. The secondary structure was estimated by curve fitting to 33 reference protein spectra using the CDNN program [22].

Results

Kinetic stability. Previous experiments have already demonstrated an unexpected kinetic stability of gp36C [13]. To assess the resistance of gp36C to irreversible denaturation in more detail, we measured the residual enzymatic activity after exposure to varying heat treatments. The results show an atypical kinetic behaviour (Fig. 2). At temperatures below 75 °C, longer thermal treatments did not result in a gradual loss of activity, but in irregular fluctuations. Above 75 °C the observed kinetic data fit an exponential first-order model ($y = e^{-kt}$) with k as a rate constant (Fig. 2). The corresponding k values of 75, 85 and 95 °C (0.124 h^{-1}, 0.284 h^{-1} and 0.595 h^{-1}, respectively) were very low and correlated with the Arrhenius equation ($k = Ae^{-Ea/RT}$) ($R^2 = 0.9997$). Complete inactivation of gp36C only occurred after 8 h at 95 °C or 10 h at 85 °C. These extended data clearly confirm an exceptional thermoresistance of gp36C, although an irregular factor seems to influence the behaviour at lower temperatures.

Aggregation of gp36C. Aggregation of gp36C can be observed macroscopically at high concentrations after a heat treatment at 55 °C for 3 h. Therefore, aggregation conditions were studied in more detail by UV-VIS spectrophotometry to asses the influence of aggregation on the kinetic data. Figure 3 clearly shows the influence of the temperature of the heat treatment on aggregation of

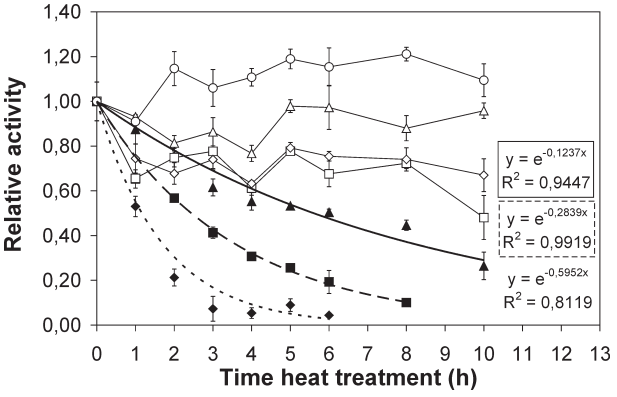

Figure 2. Kinetic stability of gp36C. The residual activity of gp36C was measured at 25 °C after a heat treatment for prolonged periods at 35 °C (open circles), 45 °C (open triangles), 55 °C (open diamonds), 65 °C (open squares), 75 °C (filled triangles), 85 °C (filled squares) and 95 °C (filled diamonds). Residual activities are represented relative to activity at 25 °C. All values are averages from triplicate experiments. The standard deviations are indicated. Data of 75, 85 and 95 °C are fit with an exponential model. Irregular fluctuations are observed at lower temperatures.

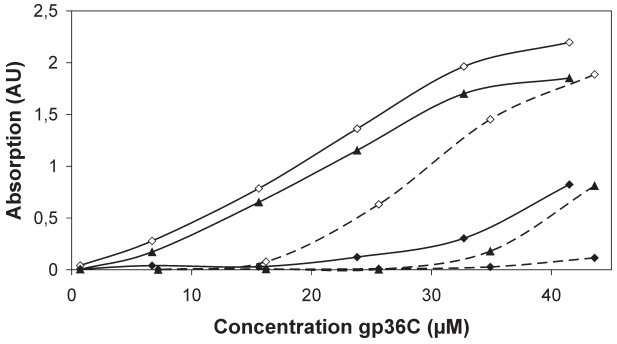

Figure 3. Aggregation effects for gp36C using UV-VIS spectrophotometry. Absorption at 350 nm was measured for gp36C at 25 °C after heat treatment at 55 °C (open diamonds), 75 °C (filled triangles) and 95 °C (filled diamonds) in ENZ (full lines) and PBHS buffer (dashed lines) for a dilution series between 1 and 45 μM. More aggregation is observed at 55 °C than at 75 or 95 °C in all tested conditions and is dependent on protein concentration.

gp36C at concentrations between 1 and 45 μM in ENZ buffer. No aggregation was observed at 25 °C. However, gp36C aggregated extensively during a treatment at 55 °C, but aggregation decreased again at 75 °C and more so at 95 °C. This behaviour is atypical since, generally, an opposite effect is expected.

Aggregation of gp36C could not be observed at 0.56 μM, the concentration used in the kinetic assay, because it is below the aggregation detection limit (~5 μM). These data and the kinetic stability assay suggested that irreversible denaturation of gp36C is influenced by aggregation at lower temperatures, but by raising the temperatures, thermal irreversible degradation exponentially becomes the most influential parameter.

Thermodynamic stability. To assess whether gp36C is also thermodynamically stable, it was analyzed by DSC. Calorimetric measurements of the thermal unfolding of gp36C (15 μM/30 μM), initially performed in ENZ buffer, revealed an irreversible and irregular exothermic peak from 40 °C (Fig. 4a). This exothermic peak is consistent with the protein aggregation, observed by UV-VIS spectrophotometry under the same conditions (Fig. 3). However, when the buffer was replaced by PBHS, gradual heating of gp36C (15 μM) resulted in a reversible, endothermic unfolding transition at T_m = 50.2 °C (Fig. 4b). The calorimetric heat of the first scan ($\Delta H_{cal} = 6.86 \times 10^4$ cal mol^{-1}) was clearly higher than that of the second, third and fourth scan, indicating that a small fraction of the total protein amount denatured irreversibly during the sequential scans. The symmetric profiles of the transition peaks fit the Van 't Hoff relation, with a related heat (ΔH_{VH}) of 6.19×10^4 cal mol^{-1}. The ratio of $\Delta H_{cal}/\Delta H_{VH}$ agrees well with a two-state-like transition model for protein unfolding. A different aggregation behaviour of gp36C in PBHS compared with ENZ buffer could be confirmed by UV-VIS spectrophotometry: aggregation still

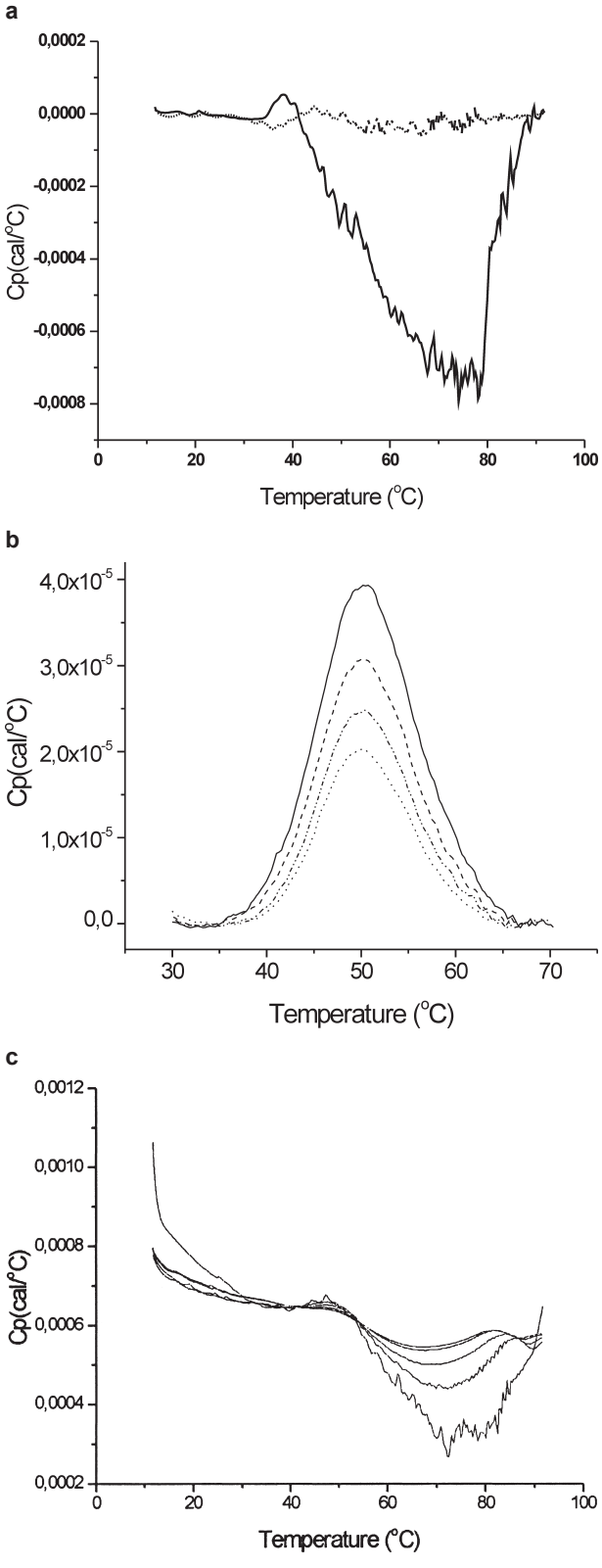

Figure 4. DSC analysis of gp36C. The heat capacity in ENZ buffer with 15 μM gp36C (*a*), PBHS with 15 μM gp36C (*b*) and PBHS with 30 μM gp36C (*c*) was measured as a function of temperature. An endothermic, reversible transition is observed in *b* in contrast with an exothermic, irreversible aggregation of gp36C in *a* and *c*. Two (*a*), four (*b*) and seven (*c*) sequential scans are shown.

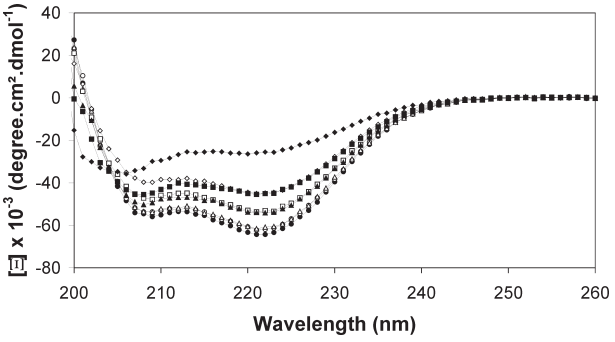

Figure 5. CD analysis of gp36C. Different CD spectra of gp36C after thermal treatment at 25 °C (filled circles), 35 °C (open circles), 45 °C (open triangles), 55 °C (open diamonds), 65 °C (open squares), 75 °C (filled triangles), 85 °C (filled squares) and 95 °C (filled diamonds).

occurred in PBHS, but to a significantly lower extent compared with the ENZ buffer (Fig. 3). The threshold concentration for aggregation detection is approximately 15 μM. Accordingly, DSC analysis of gp36C in PBHS at concentrations above 15 μM resulted in irregular, exothermic peaks as observed with the ENZ buffer (Fig. 4c). However, less extensive aggregation in PBHS was unexpected, since the solubility of a protein generally decreases at a higher ionic strength (0.5 M NaCl in PBHS) due to shielding of charges and the corresponding salting-out effect.

Although T4 lysozyme is not kinetically stable (complete inactivation after 5 min at 75 °C [16]), its thermodynamic stability (T_m = 64.7 °C at pH 6.5, $\Delta H_{cal} = 12.5 \times 10^4$ cal mol^{-1} [23]) is higher than that of gp36C (T_m = 50.2 °C at pH 7.4, $\Delta H_{cal} = 6.86 \times 10^4$ cal mol^{-1}). T4 lysozyme is co-operatively folded in an apparent two-state ($N \leftrightarrow U$) transition as well, despite its bipartite structure [20].

Structural analysis. Since DSC analysis showed reversible unfolding of gp36C in PBHS, CD analysis of gp36C was performed to gain insight into its secondary structure after renaturation. CD spectra of gp36C samples were recorded at room temperature after a 3-h heat treatment (between 25 and 95 °C). CD spectra recorded in the ENZ buffer were not successful due to the aggregation discussed above and concomitant loss of the signal. On the other hand, measurements in PBHS revealed spectra with characteristic minima at 207 and 222 nm, indicating a high α helicity of gp36C (Fig. 5). The varying amplitude of the curves can be attributed to irreversible denaturation of gp36C, which was also observed in kinetic stability assays after the same heat treatments. Deconvolution analysis of the different CD spectra was performed to estimate percentages of secondary structure after the heat treatments and renaturation at room temperature (Table 1). Gp36C has a very high α helicity (~93%) similar to that of T4 lysozyme [17, 18]. Other minor fractions are β turns (4%), parallel

Table 1. CDNN analysis of CD spectra of gp36C.

Temperature (°C)	α helix %	Random coil %	β turn %	Anti-parallel %	Parallel %	Sum %
25	93.0	4.2	4.0	0.1	3.0	104.3
35	92.1	4.8	4.3	0.1	3.2	104.5
45	91.5	5.2	4.7	0.2	3.2	104.8
55	79.0	13.3	9.3	0.9	4.3	106.8
65	86.9	8.3	6.8	0.3	3.6	105.9
75	85.5	8.7	7.9	0.3	3.3	105.7
85	75.9	13.9	12.2	0.7	3.6	106.3
95	36.3	30.3	26.2	4.6	3.9	101.3

Estimation of the percentages of secondary-structure fractions of gp36C after a 3-h thermal treatment at different temperatures are based on 33 reference protein spectra with known crystal structure [22]. The average prediction error for the secondary-structure total content of a protein contained in the program database is 6.45%. The summed proportions fall within the prediction error.

β sheets (3%) and random coils (4%). Samples heated at 35 and 45 °C generally retained the same secondary-structure fractions. Aliquots of gp36C heated at temperatures above T_m = 50.2 °C showed an altered secondary structure, although the α helix content was still high (between 75.9 and 86.9%) from 55 to 85 °C. At 95 °C, the CD spectrum was drastically transformed and the α helix content dropped to 36.3%. Increased proportions of random coils and β turns compensated for these drops. Remarkably, the parallel β sheet fraction remained equal after all treatments. The predicted catalytic triad is embedded in this parallel β sheet fraction (Fig. 1).

Discussion

In considering protein stability, a clear distinction has to be made between thermodynamic stability and kinetic stability. Thermodynamic stability deals with the equilibrium between the native (N) and the unfolded (U) state of a protein and is correlated with the energy difference (ΔG_D) between the N and U state. Kinetic stability refers to the resistance of a protein to irreversible denaturation, which is coupled to the U state. Lavigne et al. [13] reported an exceptionally high kinetic stability for recombinant gp36C, which still retained over 50% residual activity after 1 h at 100 °C. On the other hand, T4 lysozyme (to which gp36C has 44% sequence similarity and 27% sequence identity) is completely inactivated after 5 min at 75 °C [16]. Such a high kinetic stability has not yet been described before for any other phage muralytic enzyme.

Here we show that gp36C behaves thermodynamically as a normal mesophilic protein and is thermodynamically

less stable than T4 lysozyme, but its stability can be attributed to an exceptionally high thermoresistance with extremely low rates of irreversible denaturation.

Moreover, the kinetic behaviour is influenced by unusual aggregation phenomena, which are more pronounced at 55 °C than at 75 °C and even less pronounced at 95 °C in both buffers. This was unexpected because, normally, the rate of aggregation is slower at lower temperatures since it has to compete with protein folding. Therefore, we suggest that here, aggregation is not caused by the non-specific association of hydrophobic surfaces that are exposed after denaturation, but is driven by sequence-specific oligomerization. There is increasing evidence that protein aggregation often relies on a specific primary sequence [24, 25] and very short stretches of amino acids can cause precipitation [26]. These oligomers can protect gp36C against irreversible denaturation and enhance thermoresistance [27]. According to this hypothesis, higher temperatures in the kinetic stability assay will result in a gradual loss of these sequence-specific oligomers and more irreversible denaturation.

Furthermore, both DSC and CD analysis showed that unfolding of gp36C is reversible. Even after long heat treatments at high temperatures, gp36C can regain its intact secondary structure (up to 45 °C) or its partially refolded structure (between 55 and 85 °C).

Proteins are maximally evolved to perform their biological function. Gp36C is a C-terminal muralytic domain of gp36, which is predicted as an internal virion protein of ϕKMV [12]. We previously suggested that gp36 degrades the peptidoglycan locally to facilitate DNA entry during infection [13]. In bacteriophage T7, a close relative, this function is attributed to gp16. The high thermoresistance of gp36C is in agreement with the 'folding carpenter's rule model' suggested by Molineux [28] for gp16 of bacteriophage T7. Gp16 is a large internal virion protein (1318 amino acids) that is part of the T7 injection needle. A T7 virion contains an estimated four copies [29]. To extrude from the internal core of the virion capsid during infection, they must transiently unfold to allow passage of the large proteins through the restricted head-tail connection of the phage particle (2.7 nm). Gp16 has a high α-helical (50%) and random-coil (30%) content according to secondary-structure prediction tools. Molineux [28] suggests that gp16 resembles a 'folding carpenter's rule', with each segment of the rule corresponding to an α helix. Like a 'carpenter's rule', gp16 molecules unfold to long linear molecules to exit the capsid. However, they retain enough structural information to refold rapidly in the periplasm. There, they can degrade the host cell wall peptidoglycan and integrate in the inner membrane. We suggest a similar model for gp36, although we propose that gp36 does not exit one by one, but in a linear oligomerized form of unfolded proteins. The existence of an *in vivo* functional unfolded state of gp36 (or gp16) may explain the necessity of a strong resistance to irreversible denaturation coupled to this state.

The normal thermodynamic stability, the high thermoresistance, the putative oligomerization and the capability of gp36C to refold easily all support this model. According to this hypothesis, high thermoresistance could be a common property of structural muralytic domains of other members of the T7 supergroup like T3, SP6, K1-5 and ϕYe03-12. Moak and Molineux [5] have already demonstrated the presence of peptidoglycan hydrolytic activity associated with all these virions. The internal virion-protein-encoding genes of these phages have a similar arrangement. However, most members of the T7 supergroup have an N-terminally localized muralytic domain instead of the C-terminal domain in ϕKMV gp36, which is encoded by the upstream gene compared with T7. Furthermore, the size of ϕKMV gp36 is similar to the T7 internal virion protein gp15 and not to the downstream-encoded gp16. To date, *Salmonella typhimurium* bacteriophage SP6 and *E. coli* phage K1-5 are the only other phages known to have the same module arrangement as observed in ϕKMV. The copy number of T7 gp15 is estimated to be eight [30] compared to four for gp16 [29], but is still unknown for ϕKMV gp36. Regardless of whether gp36 is more functionally related to T7 gp15 or gp16 internal virion proteins, the hypothesis that gp36 leaves the capsid as an oligomerized unfolded structure remains valid, as long as the oligomer dimensions are compatible with passage through the restricted head-tail connection. However, the actual nature of the oligomer still has to be elucidated.

Gp36C offers interesting perspectives both in applications and as a fundamental research topic, in view of its role in the phage infection process and its similarity to the well-known but thermosensitive T4 lysozyme. Phage-encoded muralytic enzymes (lysins) have recently been considered for use as antimicrobial agents to control pathogenic bacteria [11, 31]. Fischetti and coworkers [32, 33] applied lysins externally to bacteria and observed that the bacteria were killed seconds after contact. Thermoresistant lysins such as gp36C offer an additional advantage to develop novel tools based on phage lysins, due to their stability and thus good storage possibilities.

Acknowledgements. The authors thank C.W. Michiels (Laboratory of Food Microbiology, Katholieke Universiteit Leuven, Leuven, Belgium) for the use of the Bioscreen Microbiology Reader. E. Lorent and M. Gérard (Laboratory of Biomolecular Dynamics, Katholieke Universiteit Leuven, Leuven, Belgium) are gratefully acknowledged for their helpful discussions and technical assistance concerning CD spectra and UV-VIS measurements, respectively. The work was financially supported by the research council of the KULeuven grants OT/04/30 and OT/05/45 and the Flemish FWO research grant G.0308.05. Y.B. holds a predoctoral fellowship of the 'Instituut voor de aanmoediging van Innovatie door Wetenschap en Technologie in Vlaanderen' (I.W.T., Belgium). R.L. and K.H. hold a postdoctoral fellowship of the 'Fonds voor Wetenschappelijk Onderzoek-Vlaanderen' (FWO-Vlaanderen, Belgium).

1 Delbrück, M. (1940) The growth of bacteriophage and lysis of the host. J. Gen. Physiol. 23, 643–660.
2 Kao, S.-H. and McClain, W. H. (1980) Baseplate protein of bacteriophage T4 with both structural and lytic function. J. Virol. 34, 95–103.
3 Nakagawa, H., Arisaka, F. and Ishii, S. (1985) Isolation and characterization of the bacteriophage T4 tail-associated lysozyme. J. Virol. 54, 460–466.
4 Moak, M. and Molineux, I. J. (2000) Role of the gp16 lytic transglycosylase motif in bacteriophage T7 virions at the initiation of infection. Mol. Microbiol. 37, 345–355.
5 Moak, M. and Molineux, I. J. (2004) Peptidoglycan hydrolytic activities associated with bacteriophage virions. Mol. Microbiol. 51, 1169–1183.
6 Kao, S. H. and McClain, W. H. (1980) Baseplate protein of bacteriophage T4 with both structural and lytic functions. J. Virol. 34, 95–103.
7 Rydman, P. S. and Bamford, D. H. (2002) The lytic enzyme of bacteriophage PRD1 is associated with the viral membrane. J. Bacteriol. 184, 104–110.
8 Kivelä, H. M., Daugelavičius, R., Hankkio, R. H., Bamford, J. K. and Bamford, D. H. (2004) Penetration of membrane-containing double-stranded DNA bacteriophage PM2 into *Pseudoalteromonas* hosts. J. Bacteriol. 186, 5342–5354.
9 Daugelavičius, R., Cvirkaite, V., Gaidelyte, A., Bakiene, E., Gabrenaite-Verkhovskaya, R. and Bamford, D. H. (2005) Penetration of enveloped double-stranded RNA bacteriophages phi13 and phi6 into *Pseudomonas syringae* cells. 79, 5017–5026.
10 Kenny, J. G., McGrath, S., Fitzgerald, G. F. and van Sinderen, D. (2004) Bacteriophage Tuc2009 encodes a tail-associated cell wall-degrading activity. J. Bacteriol. 186, 3480–3491.
11 Takác, M. and Bläsi, U. (2005) Phage P68 virion-associated protein 17 displays activity against clinical isolates of *Staphylococcus aureus*. Antimicrob. Agents Chemother. 49, 2934–2940.
12 Lavigne, R., Burkal'tseva, M. V., Robben, J., Sykilinda, N. N., Kurochkina, L. P., Grymonprez, B., Jonckx, B., Krylov, V. N., Mesyanzhinov, V. V., Volckaert, G. (2003) The genome of bacteriophage phiKMV, a T7-like virus infecting *Pseudomonas aeruginosa.* Virology 312, 49–59.
13 Lavigne, R., Briers, Y., Hertveldt, K., Robben, J. and Volckaert, G. (2004) Identification and characterization of a highly thermostable bacteriophage lysozyme. Cell. Mol. Life Sci. 61, 2753–2759.
14 Lavigne, R., Noben, J.-P., Hertveldt, K., Ceyssens, P.-J., Briers, Y., Dumont, D., Roucourt, B., Krylov, V. N., Mesyanzhinov, V. V., Robben, J., Volckaert, G. (2006) The structural proteome of *Pseudomonas aeruginosa* bacteriophage ϕKMV. Microbiol. SGM 152, 529–534.
15 Wozniak, J. A., Zhang, X.-J., Weaver, L. H. and Matthews, B. W. (1994) Structural and genetic analysis of the stability and function of T4 lysozyme. In: Bacteriophage T4. (Karam, J. D., Ed.), pp. 332–342. American Society for Microbiology, Washington D. C.
16 Tsugita, A. and Inouye, M. (1968) Purification of bacteriophage T4 lysozyme. J. Biol. Chem. 243, 391–397.
17 Remington, S. J., Anderson, W. F., Owen, J., Ten Eyck, L. F., Grainger, C. T and Matthews, W. (1978) Structure of the lysozyme from bacteriophage T4: an electron density map at 2.4 Å resolution. J. Mol. Biol. 118, 81–98.
18 Weaver, L. H. and Matthews, B. W. (1987) Structure of bacteriophage T4 lysozyme refined at 1.7 Å resolution. J. Mol. Biol. 193, 189–199.
19 de Groot, B. L., Hayward, S., van Aalten, D. M., Amadei, A. and Berendsen, H. J. (1998) Domain motions in bacteriophage T4 lysozyme: a comparison between molecular dynamics and crystallographic data. Proteins 31, 116–127.
20 Llinás, M. and Marqusee, S. (1998) Subdomain interactions as a determinant in the folding and stability of T4 lysozyme. Prot. Sci. 7, 96–104.
21 Llinás, M., Gillespie, B., Dahlquist, F. W. and Marqusee, S. (1999) The energetics of T4 lysozyme reveal a hierarchy of conformations. Nat. Struct. Biol. 6, 1072–1078.
22 Bohm, G., Muhr, R. and Jaenicke, R. (1992) Quantitative analysis of protein far-UV circular dichroism spectra by neural networks. Prot. Eng. 5, 191–195.
23 Matthews, B. W., Nicholson, H. and Becktel, W. J. (1987) Enhanced protein thermostability from site-directed mutations that decrease the entropy of unfolding. Proc. Natl. Acad. Sci. USA 84, 6663–6667.
24 Chiti, F., Stefani, M., Taddei, N., Ramponi, G. and Dobson, C. M. (2003) Rationalization of the effects of mutations on peptide and protein aggregation. Nature 424, 805–808.
25 Salvador, V. (2005) Sequence determinants of protein aggregation: tools to increase protein solubility. Microb. Cell. Fact. 4, 11–18.
26 Ventura, S., Zurdo, J., Narayanan, S., Parreno, M., Mangues, R., Reif, B., Chiti, F., Giannoni, E., Dobson, C. M., Aviles, F. X., Serrano, L. (2004) Short amino acid stretches can mediate amyloid formation in globular proteins: the Src homology 3 (SH3) case. Proc. Natl. Acad. Sci. USA 101, 7258–7263.
27 Kil, Y. V., Glazunov, E. A. and Lanzov, V. A. (2005) Characteristic thermodependence of the RadA recombinase from the hyperthermophilic archaeon *Desulfurococcus amylolyticus*. J. Bacteriol. 187, 2555–2557.
28 Molineux, I. J. (2001) No syringes please, ejection of phage T7 DNA from the virion is enzyme driven. Mol. Microbiol. 40, 1–8.
29 Kemp, P., Garcia, L. R. and Molineux, I. J. (2005) Changes in bacteriophage T7 virion structure at the initiation of infection. Virology 340, 307–317.
30 Cerritelli, M. E., Trus, B. L., Smith, C. S., Cheng, N., Conway, J. F. and Steven, A. C. (2003) A second symmetry mismatch at the portal vortex of bacteriophage T7: 8-fold symmetry in the procapsid core. J. Mol. Biol. 327, 1–6.
31 Fischetti, V. A. (2001) Phage antibacterials make a comeback. Nat. Biotechnol. 19, 734–735.
32 Loeffler, J. M., Nelson, D. and Fischetti, V. A. (2001) Rapid killing of *Streptococcus pneumoniae* with a bacteriophage cell wall hydrolase. Science 294, 2170–2172.
33 Nelson, D., Loomis, L. and Fischetti, V. A. (2001) Prevention and elimination of upper respiratory colonization of mice by group A streptococci by using a bacteriophage lytic enzyme. Proc. Natl. Acad. Sci. USA 98, 4107–4112.